Soft Matter

PAPER

# Predation with the tongue through viscous adhesion, a scaling approach

Cite this: DOI: 10.1039/c7sm00134g

Maurine Houze* and Pascal Damman

Received 19th January 2017,
Accepted 30th January 2017

DOI: 10.1039/c7sm00134g

rsc.li/soft-matter-journal

Some predators, mainly lizards and amphibians, capture their prey with their tongue. The process of capture involves strong adhesion mechanisms to overcome inertial forces that should be related to a viscous mucus produced at the tongue tip. A scaling model of prey capture independent of the anatomic details of the animals is developed from a study of viscous adhesion with a probe-tack geometry. This model is then successfully applied to describe the nonlinear evolution of the maximum prey size with the predator length for chameleons. This approach of prey capture defines a new framework that should help biophysicists and biologists to study more quantitatively the adhesion mechanisms for various animals and biological processes.

## 1 Introduction

Understanding the physical mechanisms that underlie the behavior of animals is a real challenge in biology. The validity of a hypothesized model is generally demonstrated through the comparison between the predictions of the model and experimental observations. These systematic observations are often generated in the laboratory with animals in captivity and require a long period of acclimatation with tedious training. This procedure has a major drawback: you are never certain that these data are really representative of the *in vivo* behavior. Here, we suggest the preferential use of data directly recorded in the natural habitat of animals and the use of scaling law models. To validate this approach, we focused on a ''case study'', predation with the tongue, a methodology used mainly by lizards and amphibians,[1] and more specifically by chameleons since there is literature available for this species. Chameleons capture prey by shooting them with their tongue at very high acceleration, $\sim$ 40 g.[2–4] The prey should obviously stick to the tongue during all the accelerated phase, *i.e.* adhesion should overcome the large inertial forces at play. The maximum prey size that could be captured is directly determined by this adhesion strength. Regarding the mechanisms of adhesion, this mode of capture imposes constraints. It should work in a wet environment, for any type of surface (*e.g.*, insect cuticles are often superhydrophobic) and be easily reversible (*i.e.*, detachment should occur in the predator mouth to allow ingestion), which is not compatible with capillary adhesion. In addition, these animals have highly viscous mucus produced by specific glands located at the tongue tip.[4] These constraints strongly suggest that the adhesion mechanism is related to the viscous flow in the thin fluid layer squeezed between the tongue and the prey surface during the contact.

To build a scaling law model of the capture, we modeled the adhesion process using a minimal system: a Newtonian fluid layer with a constant thickness confined between two flat and smooth surfaces. For this purpose, we start with an experimental/theoretical study of viscous forces generated during the separation of the two surfaces at a constant velocity $v$ using a probe-tack geometry.[5,6] This study yields the relations between the various experimental parameters (contact area $\Sigma$, fluid viscosity $\eta$, and layer thickness $h_0$) and the adhesion force that could be sustained by the viscous fluid. Since the maximum adhesion force is observed during the first stages of retraction, we do not however consider the fingering instability observed in the very late stages when the adhesion forces become negligible.[7–9]

Finally, we use these relations to derive a scaling law model of the global capture which yields the evolution of the maximum prey size with predator size that could be compared to the nonlinear laws found in the literature[10,11] ($L_{\text{prey}} \propto L^{1.4}$, with $L_{\text{prey}}$ and $L$ being the maximum prey and chameleon sizes, respectively).

In addition, this study should also give an insight into biological adhesion mechanisms. Controlling adhesion is an essential issue in the living world, either for locomotion or to design permanent attachment devices. This topic has been the subject of intense research activity over the last few years for understanding the adhesion mechanisms in various biological models and to translate this knowledge into the design of new adhesive materials. Various mechanisms have been proposed to describe the adhesion strength between two surfaces, they can be separated into dry *vs.* wet adhesion.[12–14] Dry adhesion is

*Laboratoire Interfaces & Fluides Complexes, Université de Mons, 20 Place du Parc, B-7000 Mons, Belgium. E-mail: pascal.Damman@umons.ac.be*

generally invoked to explain the ability of a gecko to climb smooth surfaces. In this case, the adhesion is mediated through vdW forces between the gecko pads and the surface.[15] To optimize the contact area, the pad is divided into a myriad of small seta that deform to follow the substrate roughness. Small insects climb walls and ceilings *via* a wet adhesion mechanism relying on capillary forces. The fluid squeezed between both surfaces generates a depression due to the negative Laplace pressure created by the meniscus. A strong adhesion is obviously achieved when the liquid and the solid have a strong affinity. Some more exotic mechanisms are also invoked to explain specific biological attachment ability, mechanical interlocking for the dragonfly[16] and suction forces for the octopus.[13,14] Adhesion from forces generated through flows in viscous fluids is however conspicuously absent in the literature, despite its major role demonstrated in the locomotion of snails and tree frogs based on shear forces in a viscous mucus.[17,18]

## 2 Materials and methods

The experiments were performed using a probe-tack geometry, the system being made of two flat and parallel surfaces separated by a variable gap, $h$. The lower plate is a smooth metallic substrate while the upper plate is mounted on a moving probe attached to a compliant force gauge (maximum peak forces of 10 or 50 N). The more compliant system is obviously characterized by a greater deformability. A single experiment is conducted according to the following scheme. First, a droplet of polydimethylsiloxane (PDMS), $\eta \simeq 4$ Pa s, is initially deposited on the bottom surface. The mobile upper plate is then lowered to confine the viscous fluid between these two surfaces at an initial thickness $h_0$ close to 100 μm. Finally, the upper surface is retracted at a constant velocity of $0.01\ \text{mm s}^{-1} \leq v_0 \leq 25\ \text{mm s}^{-1}$.

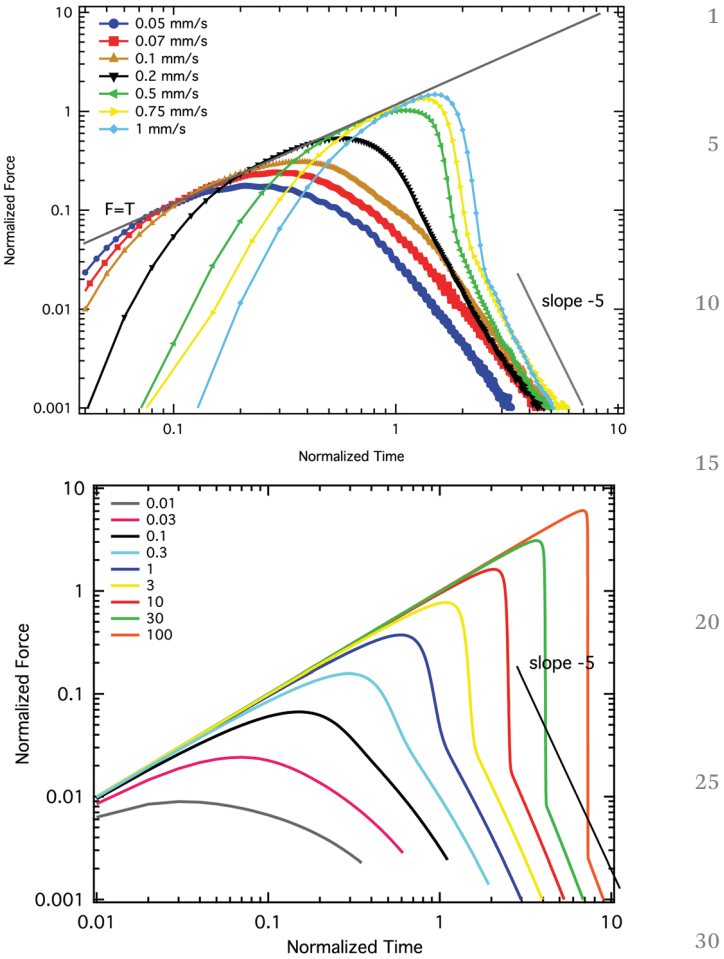


Fig. 1 Evolution of the retraction/adhesive force with time for (a) thin films of silicon oil between a metal plate and an aluminium probe (50 N force sensor, $\eta \simeq 4$ Pa s, $h_0 \simeq 100$ μm, retraction velocity as indicated) and (b) numerical solutions of eqn (2) (compliance index as indicated). The compliance number and the normalization method are explained in the text.

## 3 Results and discussion

### 3.1 Viscous adhesion using a probe-tack geometry

Selected time evolutions of the adhesion force recorded for various retraction velocities are shown in Fig. 1. After a short transient stage holding for less than 0.1 s related to the inertia of the system, all the force curves exhibit peak forces increasing with the retraction velocity, followed by a rapid decrease of the adhesion strength. A major difference in the global shape of the $\tilde{F}(T)$ curves however appears upon increasing the retraction velocity. For small and moderate velocities ($v_0 \leq 0.1\ \text{mm s}^{-1}$), we observe a maximum followed by a continuous decrease of the force according to a $T^{-5}$ power law. For large velocities ($v_0 \geq 0.2\ \text{mm s}^{-1}$), however, the forces curves exhibit a discontinuity. We observe (i) a peak force building within a very short time and increasing with the velocity; (ii) a sudden drop in the adhesive force; and (iii) a slower decrease of the force. This sudden drop is obviously reminiscent of a viscoelastic relaxation process. As suggested in ref. 5 and 6, this viscoelastic behavior should be described through a coupling between elastic deformation of the probe and the viscous flow within the thin fluid layer, produced by the retraction of the probe. Viscous adhesion is indeed a common phenomenon observed when attempting to separate two surfaces connected through a thin film of viscous fluid. Neglecting capillary forces,† the retraction of the upper surface involves an instantaneous radial flow generating a depression at the origin of the adhesive force, $F_a$. This force can be easily estimated by considering the Stokes equation, $\Delta P/R \sim \eta u/h^2$, where $u$ is the radial velocity of the fluid. From volume conservation, we convert the radial flow speed into retraction velocity, $u \sim Rv/2h$. Considering that the force is directly generated by the pressure drop, we finally get $F_a = \beta\eta\Omega^2 v/h^5$ (with $\Omega = \pi R^2 h_0$ and $\beta = 3/2\pi$).‡ In contrast, the elastic deformation of the system generates a restoring force,

† There are two forces acting on the drop: (i) the capillary force given by the surface tension and (ii) the viscous force. For highly viscous fluids and high retraction velocities, the magnitude of the viscous force ($\sim$N) is much larger than the capillary forces ($\sim 10^{-3}$ N), that can be neglected.

‡ The calculation of the force by solving explicitly the Stokes equation yields the constant $\beta$; see, for instance, J. J. Bikerman, *J. Colloid Sci.*, 1947, **2**, 163.

$F_{el} = K\Delta L$, where $K$ is the stiffness of the probe. During an experiment at constant retraction velocity, we have $F_{el} = F_a$. The change in length imposed by the retraction at constant velocity, $\Delta L = v_0 t$, can then be accounted by two processes, either a deformation of the probe system (elasticity dominated regime) or an increase of the distance $h$ between both surfaces (viscous regime). The surfaces will ultimately detach from each other, *i.e.*, for long times, the elastic deformations fully relax through the viscous flow. The transition between the elastic and viscous regimes can be defined through the dimensionless compliance index, $C = F_a/F_{el} = 3/2\pi{\cdot}\eta\Omega^2 v/Kh_0{}^6$, assuming that the characteristic change in length is given by the initial fluid thickness $h_0$. The transition between both regimes, corresponding to a sudden release of the adhesion force, should be entirely determined by this parameter. Dimensionless time and force can be built, $T = tv/h_0$ and $\tilde{F} = F/Kh_0$, helping to rationalize the plot of adhesion curves (Fig. 1). The transition time and the maximum adhesion force are obviously determined by the compliance index, $T^*(C)$ and $\tilde{F}_{max}(C)$. The dynamics of the retraction is derived according to the method first reported in ref. 5 and 6.

Considering that retraction velocities are very small compared to the sound velocity, a quasi-static approximation can be considered. The dynamics is then given by a simple balance of forces, $F_a = F_{el}$, which yields,

$$\frac{3}{2\pi}\eta\frac{\Omega^2\dot{h}(t)}{h^5} = K[vt + h_0 - h(t)] \qquad (1)$$

Considering the dimensionless variables, $T$ and $\tilde{F}$, and normalizing the distances by the initial fluid thickness, $H = h(t)/h_0$, an ODE involving the compliance index $C$, summing the various physical parameters of the system, is obtained,

$$\tilde{F} = 1 + T - H = C\frac{\dot{H}}{H^5} \qquad (2)$$

The evolution of the normalized force $\tilde{F}$ obtained numerically from eqn (2) is shown in Fig. 1 for various values of $C$. A very good agreement with the experimental curves is observed, all the characteristic features are adequately reproduced, *i.e.*, the linear increase of $\tilde{F}$ with $T$, the sudden drop in force followed by a decrease in $T^{-5}$. Interestingly, Fig. 1 also shows that the magnitude of the drop in force strongly depends on the compliance index. For small values of $C$ the sudden decrease in force even disappears completely. To build the prey capture model, we need the relation between the peak force of adhesion, $\tilde{F}_{max}$, and the different physical parameters. The global shape of the evolution of force and thickness with time is first discussed (Fig. 2). The external retraction force required to keep the retraction velocity constant first generates a quasi-instantaneous elastic deformation of the probe characterized by an elastic force that grows linearly with time, $\tilde{F} = T$, since $\Delta L = 1 - H + T \simeq T$. During this phase the fluid thickness remains very close to the initial thickness, $H \simeq 1$. After a characteristic relaxation time $T^*$, depending on $C$, the viscous flow in the fluid layer induces an increase of $H$ that releases the elasticity stored in the probe. The retraction force drops suddenly accompanied by a rapid increase of the fluid thickness, in order to follow $H \simeq 1 + T^*$ (*i.e.*, $\Delta L$ becomes negligible for $T > T^*$). As observed in the experimental and theoretical curves in Fig. 1 and 2, the dynamics is controlled by the fluid thickness as shown by the classical $T^{-5}$ dependency, observed after the sudden force drop.

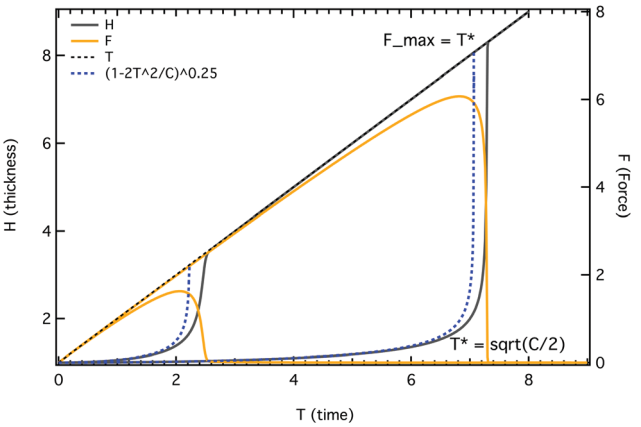


Fig. 2 Evolution of the force and thickness with time computed from eqn (2) plotted with the "small $T$" solution $H \simeq (1 - 2T^2/C)^{-1/4}$ for two values of the compliance numbers (10 and 100).

The transition between elastic and viscous regimes is fully determined by the compliance index, $C$. Larger values of $C$, *i.e.*, higher retraction velocities, yield longer transition times. In contrast, increasing the probe stiffness (smaller $C$) produces an earlier transition toward the viscous regime. These features are very well accounted by eqn (2). The evolutions of the maximal adhesion forces with $C$ are plotted in Fig. 3 for both experiments and numerical calculations. We have an excellent quantitative agreement between experiments and theory for all range of compliance numbers. It appears however that the evolution of the peak force cannot be described by a single power law, even if for large $C$'s, the data tend to follow the $\tilde{F}_{max} \sim \sqrt{C}$ law. To theoretically derive this relation, we solved eqn (2) for the short time regime, *i.e.*, a negligible increase in thickness, $H \simeq 1$ (see Fig. 2). Considering $\tilde{F} \simeq T$, the dynamics is determined by the relation, $C\dot{H}/H^5 \simeq T$. By integration of this ODE, the evolution of the normalized thickness with time is obtained,

$$H \simeq \frac{1}{(1 - 2T^2/C)^{1/4}} \qquad (3)$$

Eqn (3) adequately describes the shallow increase in thickness observed in Fig. 2 and the sudden jump observed at $T^* \simeq \sqrt{C/2}$. There are very small deviations with respect to the numerics. The divergence of the fluid thickness at $T^*$ corresponds to the maximal adhesion force given by $\tilde{F}_{max} \simeq T^* \simeq \sqrt{C/2}$. As shown in Fig. 3, the quantitative agreement with both experiments and numerics clearly improves for large $C$'s indicating that this small $T$ approximation corresponds to a $C \gg 1$ asymptotic regime. This can be accounted for by considering that the length of the plateau in $H$ is given by $T^*$ which in turn is determined by $C$. The vanishing of the force drop for small $C$ is also captured by this simplified model. At $T^*$, the jump is determined by the difference between elastic and viscous

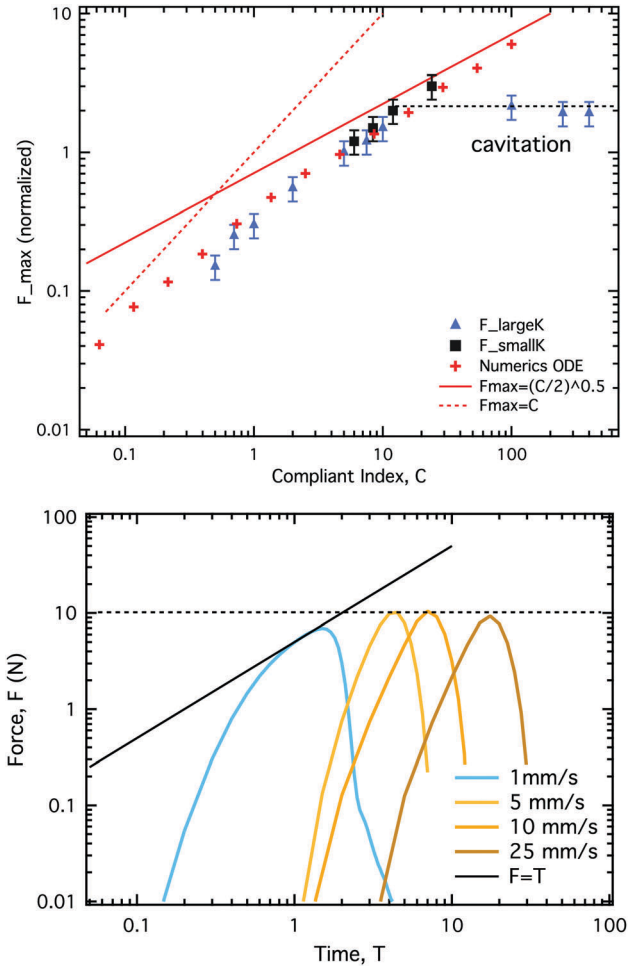


Fig. 3 (a) Evolution of the peak forces with the compliance number as measured for silicon oil experiments (10 and 50 N force sensors), computed from eqn (2) and solutions for the two asymptotic regimes (see text). (b) Force *vs.* time curves for silicon oil experiments with a high retraction velocity showing the onset of cavitation.

forces, $\Delta\tilde{F} = \tilde{F}_{el} - \tilde{F}_a$. These elastic and adhesive forces at the transition are given by $\tilde{F}_{el} = T^*$ and $\tilde{F}_a = C\dot{H}/H^5 \simeq 2T^{*2}/(1+T^*)^5$, respectively. For $T^* \ll 1$, we have $\Delta\tilde{F} \simeq T^*$, *i.e.*, the extent to which the force drop vanishes for $T^*, C \to 0$.

There is another asymptotic regime observed in Fig. 3. For very small $C$'s, the peak force tends to follow $\tilde{F}_{max} \simeq C$. In this regime, characterized by $T^* \to 0$, the approximations $\dot{H} \simeq 1$ and $H \simeq 1 + T$ are always valid since no elastic deformation of the probe is allowed. During the retraction, the peak force is almost instantaneously achieved for the initial fluid thickness giving $\tilde{F}_{max} = C\dot{H}/H^5 \simeq C$.

Finally, as shown in Fig. 3, the peak force increases with the retraction velocity (with $C$) up to a point where a constant force is observed. In fact, the largest retraction velocities (5 to 25 mm $s^{-1}$) are large enough to generate cavitation in the fluid layer. The depression induced by the Poiseuille flow becomes so large that bubbles nucleate from the dissolved gas. Considering the presence of these gas bubbles, the peak force is no more determined by the retraction velocity but by the atmospheric

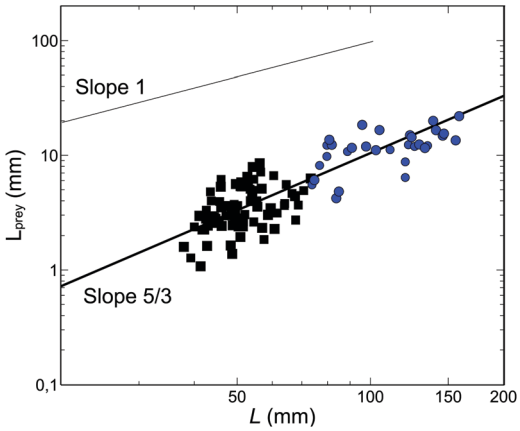


Fig. 4 Plot of the maximum prey size *versus* the chameleon size given by the snout–vent-length, $L$ determined using the $L_{prey}^{theor} \propto L^{5/3}$ scaling law (square and circle symbols correspond to ref. 10 and 11, respectively).

pressure, $F \simeq \Delta P\Sigma \simeq P_{atm}\Sigma$. For our experiments, we expect a peak force close to 10 N, in quantitative agreement with the observed plateau value in Fig. 3. This plateau pinpoints the maximum adhesion strength that can be observed for viscous adhesion. A detailed discussion of the problem of cavitation in the context of adhesion is reported in ref. 6.

### 3.2 Scaling of the prey capture mechanisms

We will now discuss the application of viscous adhesion to prey capture by animals by using their tongue. In the biological literature, chameleons clearly appear as the most extensively studied predator family. *In vivo* maximum prey sizes are plotted in Fig. 4, which shows an unexpected nonlinear evolution with the predator length.[10,11] Interestingly, we showed in a previous study that the adhesive mucus at the tongue tip behaves as a pure Newtonian fluid.[4] Regarding the wetting properties, there is unfortunately no literature about the mucus chemical composition. This point is however not crucial for viscous adhesion since the fluid is forced to spread during the impact of the tongue to form a thin layer. The viscous force is related to the radial Poiseuille flow generated during the retraction. The capillary forces produced by the meniscus are negligible, $F_{cap} < 0.1$ N. For chameleons, the compliance index is estimated to be close to 0.1§ showing that the small $C$'s asymptotic regime should hold. The maximum adhesion strength is then given by $\tilde{F}_{max} \simeq C$, which translates into $F_a \sim \eta\Sigma^2\dot{h}/h_0^3$. The key point of the model should be a clear-cut criterion determining what is an efficient prey capture. In fact, we consider that the adhesion strength should sustain inertial forces during the acceleration stage. Since the inertial forces depend on the prey mass, this criterion produces a relation between the maximum prey mass/size and the predator size (the predator size is calculated through parameters $\Sigma$, $F_t$, and $d$). The viscous adhesion is characterized by a detachment time $\tau_d$ while inertial forces

§ To estimate the order of magnitude for the compliance index, we used the following parameters found in the literature: $K \simeq 50$ N $m^{-1}$, $h_0 \simeq 10^{-4}$ m, $\eta \simeq 0.4$ Pa s, and $\Sigma \simeq 10^{-6}$ $m^2$.

only act during the duration of the acceleration stage, $\tau$. These times are equalled to give the maximum prey mass. The detachment time can be estimated through the vanishing of the adhesion force given by $\tau_d \sim h_0/\dot{h}$. Considering the expression of the adhesion force in this regime, we obtain $\tau_d \sim \eta\Sigma^2/h_0{}^2F_a$. The travel time of the prey to the predator mouth should be given by $\tau \sim d/v_p$, where $\tau$ and $d$ are the duration of the acceleration phase and the characteristic shooting distance, respectively. The prey velocity can be deduced from the dynamics of the prey–tongue system, driven by the retraction force, considering that $F_t = (m_t + m_p)a$. Since the mass of the tongue is negligible and assuming a constant acceleration, we have $F_t \simeq m_p v_p/\tau$. The velocity becomes $v_p \sim F_t\tau/m_p$, which yields $\tau \sim \sqrt{dm_p/F_t}$. The maximum prey size is then obtained by considering the critical limit $\tau_d = \tau$, considering that both retraction and adhesion forces are equal as long as the prey stays tied to the tongue, which yields,

$$m_p{}^* \sim \frac{\eta^2\Sigma^2}{h_0{}^4 dF_t} \quad (4)$$

To test this general scaling, we consider the allometric relations between the parameters and the predator size:[19,20] $\Sigma \propto L^2$,¶ $F_t \propto L^2$, and $d \propto L$. Interestingly, both mechanisms aiming to explain the retraction force produced by the chameleon tongue, *i.e.*, elastic recoil or muscular contraction, yields the same scaling in predator's size, $F_t \propto L^2$. The elastic recoil depends on the tongue stiffness and the displacement. The strength of a muscle is proportional to its cross-section. Inserting these relations into eqn (4) and considering that $L_{prey} \sim m_p{}^{1/3}$, we get the theoretical scaling $L_{prey}^{theor} \propto L^{5/3}$ that adequately explains the unexpected nonlinear scaling relation between the maximum prey size and the predator length observed for chameleons, $L_{prey} \propto L^{1.4}$ (Fig. 4).

# 4 Conclusions

A scaling model of prey capture, developed from a study of viscous adhesion, was successfully applied to describe the nonlinear evolution of the maximum prey size with the predator length for chameleons. This scaling approach could become a guideline to determine the exact nature of adhesion mechanisms for various animals and biological processes. For instance, some animals use viscous forces for locomotion. Tree frogs use structured toe pads to climb on smooth tree trunks.[18] On dry surfaces, these toe pads promote adhesion *via* their deformation to improve foot–surface contact and through the shear stress produced in the thin layer of viscous mucus during climbing.[21] Applying the proposed framework to study the locomotion of tree frogs could be a very interesting challenge.

# Acknowledgements

The authors thanks Fabian Brau, Cyprien Gay and Vincent Bels for fruitful discussions. This work was supported by the ARC Mecafood project (UMONS) and the PDR project ''Capture biomimétique de fluides'' of the FRS-FNRS.

# References

1 K. Schwenk, *Feeding: Form, Function and Evolution in Tetrapod Vertebrates*, Academic Press, 2000.
2 P. C. Wainwright, D. M. Kraklau and A. F. Bennett, *J. Exp. Biol.*, 1991, **159**, 109.
3 C. V. Anderson and S. M. Deban, *Proc. Natl. Acad. Sci. U. S. A.*, 2010, **107**, 5495.
4 F. Brau, D. Lanterbecq, L. Nastasia Zghikh, V. Bels and P. Damman, *Nat. Phys.*, 2016, **12**, 931.
5 M. Tirumkudulu, W. B. Russel and T. J. Huang, *Phys. Fluids*, 2003, **15**, 1588.
6 S. Poivet, F. Nallet, C. Gay, J. Teisseire and P. Fabre, *Eur. Phys. J. E: Soft Matter Biol. Phys.*, 2004, **15**, 97.
7 D. Derks, A. Lindner, C. Creton and D. Bonn, *J. Appl. Phys.*, 2003, **93**, 1557.
8 A. Lindner, D. Derks and M. J. Shelley, *Phys. Fluids*, 2005, **17**, 072107.
9 J. Nase, D. Derks and A. Lindner, *Phys. Fluids*, 2011, **23**, 123101.
10 G. J. Measey, A. D. Rebelo, A. Herrel, B. Vanhooydonck and K. A. Tolley, *J. Zool.*, 2011, **285**, 247.
11 F. Kraus, A. Medeiros, D. Preston, C. E. Jarnevich and G. H. Rodda, *Biol. Invasions*, 2012, **14**, 579.
12 S. Gorb, *Philos. Trans. R. Soc., A*, 2008, **366**, 1557.
13 L. Heepe and S. Gorb, *Annu. Rev. Mater. Res.*, 2014, **44**, 14.1.
14 Z. Gu, S. Li, F. Zhang and S. Wang, *Adv. Sci.*, 2016, **3**, 1500327.
15 K. Autumn, Y. A. Liang, S. T. Hsieh, W. Zesch and W. P. Chan, *Nature*, 2000, **405**, 681.
16 S. N. Gorb, *Proc. R. Soc. London, Ser. B*, 1999, **266**, 525.
17 E. Lauga and A. E. Hosoi, *Phys. Fluids*, 2006, **18**, 113102.
18 G. Hanna and W. J. Barnes, *J. Exp. Biol.*, 1991, **155**, 103.
19 T. A. McMahon and J. T. Bonner, *On size and life*, Scientific American Library, 1983.
20 K. Schmidt-Nielsen, *Scaling: why is animal size so important?* Cambridge University Press, 1984.
21 R. Gupta and J. Frechette, *Langmuir*, 2012, **28**, 14703.

¶ The scaling of the contact area is fully determined by the chameleon size. In fact, since we estimate the maximum prey size that could be captured, it is implicitly assumed that the prey size is much larger than the length of the tongue tip.